



Published in final edited form as:

Gastroenterology. 2023 July ; 165(1): 228–243.e2. doi:10.1053/j.gastro.2023.03.235.

The epigenetic reader, BRD2, mediates cholangiocyte senescence via interaction with ETS1

Jeong-Han Kang,
Patrick L. Splinter,
Christy E. Trussoni,
Nicholas E. Pirius,
Gregory J. Gores,
Nicholas F. LaRusso,
Steven P. O'Hara*

Division of Gastroenterology and Hepatology, Mayo Clinic, Rochester, MN, USA.

Abstract

Background & Aims: We reported that cholangiocyte senescence, regulated by the transcription factor, ETS1, is a pathogenic feature of Primary Sclerosing Cholangitis (PSC). Furthermore, Histone 3 Lysine 27 is acetylated at senescence-associated loci. The epigenetic readers, bromodomain and extra-terminal domain (BET) proteins, bind acetylated histones, recruit transcription factors, and drive gene expression. Thus, we tested the hypothesis that BET proteins interact with ETS1 to drive gene expression and cholangiocyte senescence.

Methods: We performed immunofluorescence for BET proteins (BRD2 and 4) in PSC patient and mouse model liver tissue. Using Normal Human Cholangiocytes (NHC), NHC experimentally induced to senescence (NHCsen), and PSC patient-derived cholangiocytes (PSCDCs), we assessed senescence, fibroinflammatory secretome, and apoptosis following BET inhibition or RNAi depletion. We assessed BET interaction with ETS1 in NHCsen and PSC patient tissues, and the effects of BET inhibitors on liver fibrosis, senescence, and inflammatory gene expression in mouse models.

*Correspondence: Steven P. O'Hara, Ph.D., Mayo Clinic, 200 First St. SW, Rochester, MN 55905, Tel: 507-284-1006, Fax: 507-284-0762, ohara.steven@mayo.edu.

Author Contributions:

Jeong-Han Kang: Conceptualization, Investigation, Formal analysis, Writing-original draft

Patrick L. Splinter: Investigation

Christy E. Trussoni: Investigation

Nicholas E. Pirius: Investigation

Gregory J. Gores: Conceptualization, Formal analysis, Writing- review and editing

Nicholas F. LaRusso: Conceptualization, Formal analysis, Writing- review and editing

Steven P. O'Hara: Conceptualization, Supervision, Formal analysis, Writing- original draft, Writing- review and editing

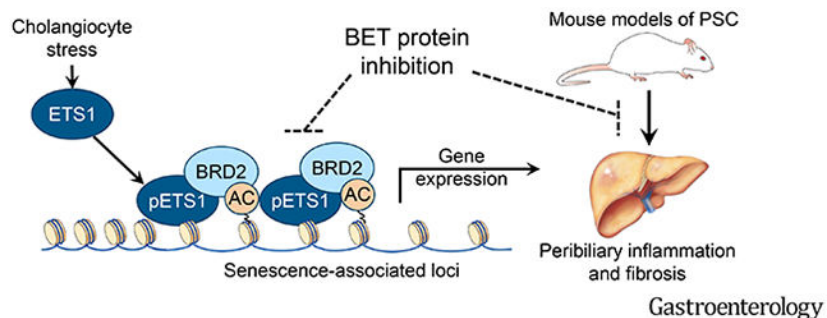
Publisher's Disclaimer: This is a PDF file of an unedited manuscript that has been accepted for publication. As a service to our customers we are providing this early version of the manuscript. The manuscript will undergo copyediting, typesetting, and review of the resulting proof before it is published in its final form. Please note that during the production process errors may be discovered which could affect the content, and all legal disclaimers that apply to the journal pertain.

We have nothing to disclose.

Results: PSC patient and mouse model tissue exhibited increased cholangiocyte BRD2 and 4 protein (~5x) compared to non-disease controls. NHCsen exhibited increased BRD2 and 4 (~2x), while PSCDCs exhibited increased BRD2 protein (~2x) relative to NHC. BET inhibition in NHCsen and PSCDCs reduced senescence markers and inhibited the fibroinflammatory secretome. ETS1 interacted with BRD2 in NHCsen and BRD2 depletion diminished NHCsen p21 expression. BET inhibitors reduced senescence, fibroinflammatory gene expression, and fibrosis in the DDC-fed and *Mdr2*^{-/-} mouse models.

Conclusion: Our data suggest that BRD2 is an essential mediator of the senescent cholangiocyte phenotype and is a potential therapeutic target for patients with PSC.

Graphical Abstract



Abstract

Background and Context: Primary sclerosing cholangitis (PSC) is an incurable cholestatic liver disease; given the morbidity and mortality of PSC, a better understanding of its pathogenesis and identification of novel therapeutic targets are needed.

New Findings: In stressed cholangiocytes, the “epigenetic reader” Bromodomain and Extraterminal Domain (BET) proteins interact with the transcription factor, ETS1, and drive cholangiocyte senescence, a prominent, likely pathologic, feature of PSC patient bile ducts.

Limitations: Our mechanistic studies use cultured cholangiocytes, patient-derived cholangiocyte organoids, and mouse models of biliary disease, none of which completely recapitulate the human condition.

Clinical Research Relevance: BET protein inhibitors improved disease in mouse models of PSC; thus, epigenetic therapy targeting BET proteins represents a novel treatment for PSC.

Basic Research Relevance: Future basic studies should focus on the non-redundant functions of individual BET proteins and their bromodomains; these additional studies will inform drug design and limit off-target effects of these epigenetic therapeutics.

Lay Summary:

The “epigenetic reader” Bromodomain and Extraterminal domain (BET) proteins drive cholangiocyte senescence, a pathologic feature of Primary Sclerosing Cholangitis (PSC); targeting BET proteins represents a novel treatment for PSC.

Keywords

Primary sclerosing cholangitis (PSC); Senescence; BET proteins; Epigenetics

INTRODUCTION

Primary sclerosing cholangitis (PSC) is an incurable cholestatic liver disease characterized by inflammation and fibrosis.^{1, 2} PSC can lead to cirrhosis and predisposes to hepatobiliary and colorectal cancer, is the 5th most common indication for liver transplantation² and has a median survival time from diagnosis to death or liver transplantation of 17 years.³ Liver transplantation is the only life-prolonging therapy.⁴ The lack of effective therapeutics is a critical unmet need. Thus, a better understanding of PSC pathogenesis and identification of novel therapeutic targets are required.

Senescence is a cellular response to chronic injury that involves cell cycle arrest and loss of proliferative capacity. Senescent cells are also resistant to apoptosis and typically express a senescence-associated secretory phenotype (SASP), characterized by increased release of cytokines, growth factors, and extracellular vesicles.⁵⁻⁷ Cholangiocytes, the epithelial cells lining bile ducts, are the target cells for several diseases, termed the cholangiopathies, including PSC. We demonstrated that cholangiocyte senescence is a prominent feature in PSC patients and animal models of PSC.⁸ We also demonstrated, *in vitro*, that persistent exposure of cholangiocytes to microbial products like lipopolysaccharide (LPS) induces senescence and the accompanying phenotypic features of apoptosis resistance, via ETS1-mediated upregulation of the anti-apoptotic protein, BCL-xL, and the senescence-associated secretory phenotype (SASP).⁸⁻¹⁰ Hence, this altered cellular state is driven by robust alterations in the senescent cholangiocyte gene expression profile. However, the precise mechanisms establishing cholangiocyte senescence-associated alterations in chromatin structure and driving gene expression remain relatively unexplored.

A growing list of transcription factors and chromatin modifying and binding proteins have been identified that collaboratively modify the senescent cell phenotype.^{11, 12} The bromodomain and extra-terminal domain (BET) protein family consists of three somatically expressed epigenetic readers (BRD2, BRD3, BRD4) essential for coordinating transcriptional programs driving development, oncogenic gene expression, and response to injury or infection.^{13, 14} All BET proteins have two tandem bromodomains (BD1 and BD2) that enable binding to acetylated lysine residues of histone tails and recruitment of transcription factors to enhancers and promoters, which, ultimately, activates RNA polymerase II machinery.^{15, 16} The functional commonalities of and differences between BD1 and BD2 remain unclear. The first generation of BET inhibitors showed equal affinity for BD1 and BD2 and revealed promising results for hematological and solid malignancies; however, side effects and short clinical responses have limited broad therapeutic application.^{14, 17} More recently, it has been shown that selective BD2 inhibitors suppressed induction of inflammatory gene expression with improved tolerability in models of inflammatory and autoimmune disease.¹³ Because our data have shown that histone acetylation is intricately involved in cholangiocyte senescence, and BET protein inhibition is

a promising therapeutic approach for inflammatory/autoimmune diseases, we explored BET protein expression and function using *in vitro* models of cholangiocyte senescence, PSC patient liver tissue, and *in vivo* models of PSC.

MATERIALS AND METHODS

This study was approved by the Mayo Clinic Institutional Review Board and Institutional Animal Care and Use Committee.

Cell culture

Normal human cholangiocytes (NHC) cell line and PSC patient-derived cholangiocytes (PSCDCs) were cultured as described.⁸ Our *in vitro* model of lipopolysaccharide (LPS)-induced senescence was performed by prolonged (8-10 day) exposure of cholangiocytes to LPS as described.⁸ On day 8, experimentally induced senescent cholangiocytes (NHCsen) were washed and complete media was added with BET inhibitors or vehicle. For cholangiocyte organoids, non-cholestatic patient or PSC patient-derived cholangiocytes were isolated from bile and mixed with matrigel (Corning); a 35 μ l droplet was placed in a prewarmed 48-well culture plate (Corning) and incubated for 15 minutes at 37°C. Additional media (240 μ l) was added to each well, then incubated at 37°C with 5% CO₂.¹⁸

RNA isolation, cDNA synthesis, and copy number quantitation

Total RNA was isolated from cholangiocyte cell lines using RNeasy Mini isolation kits (Qiagen) and 1 μ g of RNA was reverse transcribed into cDNA using Superscript III SuperMix (Thermo Scientific).

Standard curves were generated by PCR (primers in Table S1) using 1 μ g of cDNA. PCR product concentrations were determined and converted to copy numbers based on amplicon length. qPCR was performed with cDNA representing 2.5 ng of total RNA, using SYBR Green Mastermix (BioRad). The copy number of BET mRNA/ μ g of total RNA was calculated with the standard curves and normalized to 18s rRNA.

Quantitative-PCR (qPCR) analysis

Two microliters of cDNA were used for qPCR using TaqMan gene expression assays or primers (Table S1) with a QuantStudio 6 Real-Time PCR system (Applied Biosciences). Gene expression levels were determined by the 2^{-C_t} method; all experiments were performed in triplicate and normalized to 18s rRNA.

BET protein inhibitors

We used JQ1, dBET1, and GSK046 at a final concentration of 500 nM (Selleck Chemicals). JQ1 is a BET protein inhibitor with affinity for both the BD1 and BD2 domain.¹⁹ dBET1 (essentially JQ1 conjugated to cereblon E3 ubiquitin ligase ligand) is a BRD protein degrader using PROTAC technology;²⁰ GSK046 selectively inhibits the BD2 domain.²¹ NHCs experimentally induced to senescence (NHCsen) and PSC patient-derived cholangiocytes (PSCDCs) were treated with inhibitors for 48 hours. Media was collected and cells harvested for RNA or protein.

Immunoblotting

Lysates were prepared using RIPA buffer with cOmplete Protease Inhibitor (Roche). Proteins were separated by 12% SDS-PAGE, transferred to PVDF membrane, probed with antibodies (Table S2), and detected by ChemiDoc MP Imaging System (Bio-Rad) using enhanced chemiluminescence. Immunoblots were performed in triplicate; densitometric analysis, performed in ImageJ 1.42 (National Institutes of Health), is presented in Fig. S3 and 4. Briefly, band intensity of target protein was determined and normalized to β -actin band intensity from the same membrane in each independent experiment using the Plot Lanes function of ImageJ. Fold change to NHC control (set to a value of 1) was then calculated.

Immunofluorescence

Tissue sections were prepared as previously described.⁹ Briefly, slides were washed with blocking buffer (Triton X-100, 4% BSA in PBS) and incubated with primary antibodies to BRD2 (Novus Biologicals), BRD4 (Abcam), and CK7 (Santa Cruz Biotechnology) overnight at 4°C (Table S2). Slides were washed with PBS, incubated with Alexa Fluor secondary antibodies and DAPI (Life Technologies), mounted using Prolong-Gold Antifade, and analyzed with a Zeiss 780 Laser Confocal Microscope. Negative controls were performed using only secondary antibodies (data not shown). Nuclear fluorescence intensity of BET protein immunofluorescence was quantified using ImageJ. Briefly, individual cholangiocyte nuclei from six bile ducts for each condition were highlighted and integrated density was calculated. Background fluorescence from each image was calculated by measuring integrated density of an area within the image with no fluorescence and subtracted from the nuclear integrated density. Results are shown as mean \pm SEM.

Senescence-associated- β -galactosidase staining

Cells grown in 12-well plates were washed, fixed, and stained with the SA- β -gal (Cell Biolabs). Percentage of senescent cells was determined by manual counting using a 20 \times objective and bright field illumination of five randomly selected areas.

Human cytokine array

We used Proteome Profiler Human XL Cytokine Array Kit (R&D Systems) to assess NHCsen and PSCDCs secretome. The nitrocellulose membranes were incubated with 500 μ L of culture media at 4°C overnight, washed, and incubated with biotinylated antibodies. Streptavidin-HRP and chemiluminescent detection reagents were added and detected using the ChemiDoc MP Imaging System (Bio-Rad). ImageJ 1.42 was used to quantify analyte intensity. Average intensity of duplicate spots was calculated, corrected for background, and normalized to average intensity of membrane reference spots.

siRNA knockdown of BRD2 and BRD4

NHCsen were incubated with siRNAs (60 nM) to BRD2 (sc-60282) and BRD4 (sc-43639) or non-targeting siRNAs (sc-37007; Santa Cruz). Briefly, 2.5×10^5 cells were transfected with Lipofectamine 2000 (Invitrogen) and placed in complete medium for 24 hours.

Caspase 3/7 and Annexin V apoptosis assays

Apoptosis was assessed with the Caspase-Glo[®] 3/7 Assay (Promega). NHC and NHCsen were grown in 96-well plates. BET inhibitors were added for 48h, 100 μ l of Caspase-Glo[®] 3/7 was added and incubated for 2h at 37°C. Luminescence was measured using a luminometer (BioTek). Annexin V positivity was quantitated using the PE Annexin V Apoptosis Detection kit I (BD Biosciences) on MACSQuant flow cytometer (Miltenyi Biotec).

Proximity Ligation Assay (PLA)

The Sigma Doulink PLA kit was used to detect interactions between ETS1 and BRD2 or BRD4. PLAs were performed as previously described using non-disease or PSC patient-derived paraffin embedded liver sections.⁹ The slides were analyzed using a Zeiss 780 laser scanning confocal microscope. Nuclear fluorescence intensity of PLA product immunofluorescence was quantified using ImageJ 1.42 as above.

Animal experiments

C57BL/6J-*Mdr2*^{-/-} mice were a gift from Dr. Oude Elferink (Tytgat Institute). C57BL/6J (wild-type, WT) mice were obtained from Charles River. Mice were housed in a 12-hour light/dark facility with ad libitum water and food. We used female C57BL/6 for the 3,5-diethoxycarbonyl-1,4-dihydrocollidine (DDC) experiments. Mice received either a chow diet supplemented with 0.1% DDC (4 days DDC diet, 3 days standard chow) or standard chow for seven weeks. DDC diet-fed and *Mdr2*^{-/-} (*Abcb4* knockout) animals were treated by intraperitoneal injection (JQ1: 25 mg/kg) or oral administration (ABBV744: 20 mg/kg) every day for two weeks. Mice were sacrificed, and livers processed for further analysis.

Statistical analysis

Data are presented as mean \pm SD, unless otherwise noted. Student's *t*-test (2-tailed), and One-way ANOVA with Tukey's test evaluated statistical significance with GraphPad Prism 9.1 software (GraphPad Software, Inc). Within the figures, asterisks denote: *, $p < 0.05$; **, $p < 0.01$; ***, $p < 0.001$; ****, $p < 0.0001$; and n.s.: not significant.

RESULTS

Cholangiocytes express BET proteins.

We assessed the relative mRNA and protein expression of BRD2, BRD3, and BRD4 in NHC and normal mouse cholangiocytes (NMC). In both cell types, BRD2 exhibited the highest copy number ($>5.5 \times 10^4$ copies/ μ g total mRNA) while BRD3 expression was least expressed. We also found that NHC express relatively low BRD4 expression ($\sim 0.5 \times 10^4$ copies/ μ g total mRNA) compared to BRD2. In contrast, NMCs exhibited increased BRD4 mRNA expression ($\sim 4 \times 10^4$ copies/ μ g total mRNA) compared to NHC. Consistent with mRNA data, immunoblot analysis detects all three BET proteins in NHC and NMC and both the long and alternatively spliced short-form of BRD4 in both cell types; BRD2 exhibited the greatest band intensity following similar chemiluminescence detection

duration, compared to BRD3 and BRD4 (long- and short-form) (Fig. 1A and B). These results support that BRD2 is expressed in cultured cholangiocytes.

BRD2 and BRD4 protein are upregulated in cholangiocytes of PSC patients and mouse models of sclerosing cholangitis.

We next performed immunofluorescence for BRD2, 3, or 4 with cytokeratin-7 (CK7), a cholangiocyte marker in non-diseased and PSC patient liver samples. We were unable to detect BRD3 in normal or PSC patient cholangiocytes (data not shown). This result is not unexpected given the comparatively low expression of BRD3 in cultured human cholangiocytes. However, we found that both BRD2 and BRD4 protein expression (observed as nuclear puncta) were ~5-fold greater, as determined using ImageJ fluorescence intensity analyses, in cholangiocyte nuclei of PSC patients compared to non-diseased liver samples (Fig. 1 C and D). We also found that BRD2 and BRD4 were increased in cholangiocyte nuclei of DDC-fed (Fig. 1 E and F) and *Mdr2*^{-/-} mice (Fig. S1) compared to wild-type mice. These results support that BRD2 and BRD4 are expressed in cholangiocytes *in vivo*, and both are increased in biliary disease.

BRD2 expression is increased in NHCs experimentally induced to senescence (NHCsen) and PSC patient-derived cholangiocytes (PSCDCs).

We next asked whether BET protein expression is altered in senescent cholangiocytes. We found, by qPCR, that BRD2 and BRD4 expression is increased in NHCsen by ~2-fold compared to control NHC (Fig. 2A), in contrast, BRD3 expression was decreased ~30% in NHCsen compared to control NHC (Fig. S2A); hence, in additional experiments we focused on BRD2 and 4. We also found that BRD2 and 4 protein expression increased (~2-fold) in NHCsen (senescence confirmed by increased p21 expression) compared to control NHC (Fig. 2B). By immunoblot, we detected basal levels of p21 in our untreated cells, this is likely reflective of the 3-5% senescent cholangiocytes typically observed in untreated NHCs. We next assessed BRD2 and 4 expression in PSCDCs, which exhibit features consistent with senescence.²² We found, using qPCR, that BRD2 mRNA expression in PSCDCs was increased ~2.5-fold compared to NHC. In contrast, BRD4 mRNA was unchanged compared to NHC (Fig. 2C), and BRD3 was decreased approximately 50% in PSCDC compared to NHC control (Fig. S2B). We also found that BRD2 protein is increased ~2-fold, while BRD4 protein expression was reduced compared to NHC control (Fig. 2D). These results support that BRD2 and BRD4 mRNA and protein expression is elevated in NHCsen; however, in contrast to our immunofluorescence studies using PSC patient tissue, only BRD2 expression is increased in cultured PSCDCs while BRD4 is reduced. Together, these results are consistent with a role for BRD2 and/or BRD4 in cholangiocyte senescence.

Pharmacologic inhibition of BET proteins decreases cholangiocyte senescence in NHCsen and PSCDCs.

We next asked whether pharmacologic inhibition of BET proteins alters senescent cholangiocyte abundance in our cultured cholangiocyte model systems. We found that approximately 40% of the NHCsen exhibited SA- β -gal positivity (Fig 3A) and that the dual BD1 and BD2 inhibitors (JQ1 and dBET1) and the BD2 selective inhibitor (GSK046) similarly reduced the number of SA- β -gal positive cholangiocytes, supporting reduced

cholangiocyte senescence (Fig. 3A). Immunoblots showed that the inhibitors reduced BRD2 and 4 protein expression, a phenomenon previously observed in several cell types,²³⁻²⁵ and reduced expression of the senescence marker, p21 (Fig. 3B, quantitation provided in Fig S3C). Senescence and senescence reduction following BET inhibitor treatment was confirmed by western blot for p16 phospho-Ser¹⁵², a post-translationally modified form of p16 that directly interacts with CDK4 and promotes cell cycle arrest²⁶ (Fig S3 A). Similar results were found using NHC induced to senescence with H2O2 (Fig. S3B). We next assessed senescence in PSCDCs using the SA- β -gal activity assay. We found that ~40% of the PSCDCs exhibited SA- β -gal positivity, consistent with what we reported previously.²² We further found that treatment of the PSCDCs with the BET protein inhibitors reduced detection of SA- β -gal (Fig. 3C) and reduced expression of BRD2, BRD4 and the senescence marker, p21 (Fig. 3D and Fig. S3C). Next, we grew cholangiocytes isolated from control non-PSC patient bile as 3-dimensional cholangiocyte organoids in the presence or absence of LPS for 10 days and assessed senescence using the fluorescent SA- β -gal assay. We found that LPS treatment increased the number of senescent cholangiocytes (Fig. 3E). This increase in senescence was confirmed by immunoblot for p21 (Fig. 3F). We also found that each BET protein inhibitor similarly reduced SA- β -gal positivity (Fig. 3E). Immunoblots reveal that the three BET protein inhibitors significantly reduced BRD2 and 4 protein expression and reduced expression of p21 (Fig. 3F and Fig. S3C). Finally, we grew PSC patient bile-derived cholangiocyte organoids. We again observed increased SA- β -gal positivity compared to control patient-derived cholangiocyte organoids, and suppression of SA- β -gal positivity following treatment with the BET inhibitors (Fig. 3G). These PSC patient-derived cholangiocyte organoids did not expand to sufficient size to isolate protein and perform western blotting, likely due to the high number of senescent cholangiocytes in these isolated cholangiocytes (> 40%), yet, cumulatively, these results support that BET inhibitors diminish cholangiocyte senescence in our culture systems.

BET proteins interact with ETS1 and the BET protein inhibitor, JQ1, promotes senescent cell apoptosis.

In a previous study, we demonstrated that the transcription factor ETS Proto-Oncogene 1 (ETS1) is an important mediator of cholangiocyte senescence¹⁰ and promotes apoptosis resistance of senescent cholangiocytes via transcriptional upregulation of BCL-xL.⁹ Here we addressed whether ETS1 interacts with BET proteins and whether inhibition of BET proteins suppresses BCL-xL expression and promotes apoptosis. We found that NHCsen exhibit increased ETS1 expression (Fig. 4A), and that ETS1 formed an immunoprecipitable complex with both BRD2 and BRD4 in NHC. However, in NHCsen, immunoprecipitation with ETS1 resulted in ~20-fold increase in BRD2 detection, while BRD4 detection was increased less than 2-fold (Fig. 4A). These results suggest that ETS1 exhibits increased affinity for BRD2 over BRD4 in NHCsen. To determine whether BRD2 and/or BRD4 interact with ETS1 in PSC patient liver tissue, we performed proximity ligation assays. This approach further supports that both BRD2 and BRD4 interact with ETS1, yet the BRD2:ETS1 interaction is significantly increased compared to the BRD4:ETS1 interaction in PSC patient cholangiocytes (Fig. 4B). We next assessed whether BET inhibitors altered the expression of BCL-xL in both NHCsen and PSCDC. By immunoblot, we found that treatment of NHCsen and PSCDC with JQ1 reduced BCL-xL expression (35-40%) while

dBET1 and GSK046 did not significantly alter BCL-xL expression (Fig. 4C, D and Fig. S4A). We also found that JQ1 induced apoptosis in both NHCsen and PSCDCs, while dBET1 and GSK046 had no effect on caspase-3/7 detection or Annexin V positivity (Fig. 4C and D). To further define individual BET protein function in senescent cholangiocytes, we isolated SA- β GAL positive NHCsen by fluorescence-activated cell sorting (FACS) and transfected with a scrambled control, BRD2, or BRD4 siRNA. RNAi-mediated knockdown of both BRD2 and BRD4 was confirmed by qPCR and immunoblot (Fig. 4E, F and Fig. S4B). RNAi-mediated suppression of BRD2 reduced BRD2 protein by ~70% and had no effect on BRD4 expression. Conversely, RNAi-mediated suppression of BRD4 reduced BRD4 protein by ~70%, but also reduced BRD2 protein expression (~50%), suggesting that our BRD4 siRNAs may exhibit off-target effects towards BRD2 expression or that RNAi-mediated suppression of BRD4 suppresses transcription of BRD2 in NHCsen. Further immunoblots demonstrated that depletion of either BRD2 or BRD4 reduced the detection of phospho-ETS1 (~60 and <40%, respectively; Fig. 5E, F and Fig. S4B). In contrast, RNAi-mediated depletion of BRD2 decreased p21 and BCL-xL expression by greater than 75%, while BRD4 depletion reduced p21 and BCL-xL expression by <50%. This result suggests that BRD2, but not BRD4, is essential for maintaining cholangiocyte senescence.

The dual BD domain inhibitor, JQ1, and the selective BD2 domain inhibitor, GSK046, suppress the proinflammatory/fibrogenic bioactive secretome of NHCsen and PSCDCs.

Having demonstrated that BET inhibitors suppress NHCsen and PSCDC senescence, we addressed whether dual BD1/BD2 or selective BD2 BET protein inhibitors suppressed the SASP. NHCsen were treated with JQ1 (BD1 and 2 inhibitor) or the selective BD2 inhibitor, GSK046. Following a 24-hour incubation, we collected media and performed a multiplex antibody array to detect proinflammatory/fibrogenic mediators. Densitometric analysis of analyte spots revealed that NHCsen exhibited increased secretion of 22 of the 105 analytes tested (Fig. 5A). Treatment with the BET inhibitors reduced >90% of the detected analytes (Fig. 5A and S5A). We also found that the PSCDCs exhibited increased secretion of 21 of the 105 analytes tested, ~80% of which overlapped with our NHCsen secretome profile, and the majority (>90%) were reduced when PSCDCs were treated with BET inhibitors (Fig. 5B and S5B). We next assessed, by qPCR, the expression of a subset of chemokine and fibrogenic markers in NHCsen and PSCDCs. Each of the assessed chemokines and fibrogenic markers exhibited increased mRNA expression in NHCsen (~2-7-fold) and in PSCDCs (~1.5-60-fold) compared to control NHC (Fig. 5C and D). We next assessed chemokine and fibrogenic gene expression, by qPCR, in NHCsen cultured in the presence of the BET inhibitors. We found that the BET inhibitor, JQ1, reduced mRNA expression of CXCL5, CXCL10, and CXCL20 (~50-90%) but had no effect on IL-8 expression (Fig. 5E) compared to NHCsen in the absence of BET inhibitors. Treatment of NHCsen with GSK046 reduced expression of IL-8, CXCL5, and CXCL10 (~25-70%) but had no effect on CXCL20 (Fig. 5E). Both inhibitors more consistently reduced fibrogenic gene expression (~50-90%) compared to NHCsen cultured in the absence of BET inhibitors (Fig. 5E). A similar experiment was performed using PSCDCs. Again, treatment with the BET protein inhibitors reduced both the chemokine and fibrogenic gene expression (30-90%) compared to PSCDCs cultured in the absence of BET inhibitors (Fig. 5F). These results support that BET inhibitors suppress the senescent cholangiocyte SASP.

BET inhibitors diminish fibrosis in the DDC treatment and *Mdr2*^{-/-} mouse models of sclerosing cholangitis.

JQ1 was administered daily for 2 weeks via intraperitoneal injection, while the selective BD2 domain BET protein inhibitor, ABBV744, which exhibits a favorable toxicity profile in prostate xenograft models,²⁷ was administered daily for 2 weeks by oral gavage. Both the DDC-fed and *Mdr2*^{-/-} mice exhibited an increase in liver/body weight ratio, alkaline phosphatase (ALP), and alanine aminotransferase (ALT); treatment with both BET inhibitors trended toward improved liver/body weight ratio, ALP, and ALT, yet did not reach significance for either model. Picrosirius red-stained tissue sections revealed that both models exhibited increased fibrosis (Fig. 6A and B). Treatment with both JQ1 and ABBV744 significantly reduced the percentage of fibrotic area (~80% and ~50% reduction, respectively) in DDC-fed mice compared to the vehicle-treated DDC-fed group (Fig. 6A and C; Fig. S6A). Similarly, the BET inhibitors reduced Picrosirius red positivity (> 60%) compared to vehicle treated *Mdr2*^{-/-} mice (Fig. 6B and D; Fig. S6B). Biochemical assessment of hepatic fibrosis, using the hydroxyproline assay, confirmed a decrease (~35%) in total hydroxyproline concentration in the liver of JQ1- and ABBV744-treated DDC-fed and *Mdr2*^{-/-} mice compared to respective vehicle-treated controls (Fig. 6C and D). Immunoblotting further demonstrated increased alpha-smooth muscle actin (α -SMA), a marker for activated myofibroblasts, in the livers of DDC-fed and *Mdr2*^{-/-} mice, which was decreased in BET inhibitor-treated DDC-fed and *Mdr2*^{-/-} mice compared to respective vehicle treated controls (Fig. 6E and F, and Fig. S4C). These results support that inhibition of both BD1 and BD2 domains (JQ1) of BET proteins, or selective inhibition of the BET protein BD2 domain (ABBV744) reduces fibrosis in two models of sclerosing cholangitis.

BET inhibitors diminish senescence and proinflammatory gene expression in the DDC-fed and *Mdr2*^{-/-} mouse models of sclerosing cholangitis.

We next assessed whether the inhibitors reduced senescence and proinflammatory gene expression in our mouse models. Using combined CK7 immunofluorescence and p16 *in situ* hybridization, we demonstrate that both models exhibit increased senescent cholangiocytes (Fig. 7A and B). We further demonstrated reduced cholangiocyte senescence in liver tissue sections of JQ1- and ABBV744-treated DDC-fed and *Mdr2*^{-/-} mice compared to the respective vehicle treated mice (Fig. 7A and B). Quantitative PCR using mRNA derived from total liver lysates showed increased expression of the chemokines CXCL5, CCL2, and CCL20 in vehicle-treated DDC-fed and *Mdr2*^{-/-} mice compared to control mice (Fig. 7C and D). However, each chemokine was significantly reduced (~50-70%) in the JQ1 treated (Fig. 7C) compared to vehicle treated DDC-fed mice. The ABBV744-treated DDC-fed group trended toward diminished chemokine expression, yet this did not reach significance (Fig. 7C). JQ1 treated *Mdr2*^{-/-} mice also exhibited reduced expression (~50-80%) of Cxcl5 and Ccl2, while Ccl20 trended toward reduced expression. Additionally, ABBV744-treated *Mdr2*^{-/-} mice exhibited reduced expression (~50-80%) of each chemokine (Fig. 7D). We also found that both DDC-fed and *Mdr2*^{-/-} mice exhibited increased macrophage accumulation (F4/80 positivity) in the periductal areas; both JQ1 and ABBV744 diminished this macrophage accumulation (Fig. S7A and B). These results support that inhibition of BET protein BD1 and BD2 domain (JQ1), or selective inhibition of BET protein BD2 domain (ABBV744) reduces cholangiocyte senescence and markers of the cholangiocyte

SASP and diminishes macrophage accumulation to periportal regions in mouse models of sclerosing cholangitis.

DISCUSSION

The major findings reported here relate to the role of BET proteins, a family of epigenetic readers involved in transcriptional regulation, in cholangiocyte senescence and in PSC. Our data support the notion that BET protein inhibitors suppress the proinflammatory/fibrogenic cholangiocyte SASP and show for the first time that cholangiocyte BRD2 plays an essential role in maintaining cholangiocyte senescence and apoptosis resistance via direct interaction with ETS1. These findings both inform on PSC pathogenesis and have implications for development of novel pharmacotherapies for this disease.

To date, our work is the first to explore the functional role of BET proteins in intrahepatic bile duct-derived cholangiocytes and cholangiocyte senescence. All BET inhibitors decreased the number of senescent cholangiocytes in our culture systems. This supports that BET inhibition either promotes senescent cholangiocyte cell death or reduces the ongoing induction of senescence in the population. Several studies, predominantly in cancer models, demonstrated that BET protein inhibition sensitizes to apoptosis via suppressed expression of anti-apoptotic BCL2 family members.²⁸⁻³⁰ In general, senescent cells exhibit resistance to apoptosis.^{6, 31, 32} In previous work, we demonstrated that senescent cholangiocytes resist apoptosis via ETS1-mediated upregulated transcription of the anti-apoptotic BCL2 family member, BCL-xL, and BCL-xL inhibition reduced fibrosis in *Mdr2*^{-/-} mouse model of PSC.^{9, 33} Importantly, only the dual BD1/BD2 domain inhibitor, JQ1, significantly reduced BCL-xL expression and induced apoptosis. This supports that JQ1 eliminated senescent cells through induced apoptosis, and suggests a prominent role of the BD1 domain of BET proteins in regulating BCL-xL expression. Thus, while both dual BD domain inhibition via JQ1 and selective BD2 domain inhibition via GSK046 diminished senescent cholangiocyte numbers *in vitro*, these may function through distinct molecular pathways. Importantly, BET proteins have recently been shown to exhibit gene expression-independent functions. Indeed, using an unbiased high-throughput screen it was demonstrated that the BET family protein degrader (dBET, ARV825) promoted autophagy-induced cell death in senescent human diploid fibroblasts.³⁴ The proposed mechanism involves exacerbated DNA double-strand breaks, via attenuation of BET-mediated non-homologous end joining, and upregulation of autophagy-related genes. Hence, how BET inhibitors promote reduced senescent cholangiocytes in our *in vitro* and *in vivo* models remains incompletely understood, but likely involve combinatorial effects of reduced transcription, and gene expression-independent functions likely related to DNA double-strand break repair.

BET proteins are recruited to super-enhancer elements during senescence, and these elements are adjacent to SASP-related genes, suggesting a prominent role in the SASP.³⁵ Both NHCsen and PSCDCs showed increased secretion of several proinflammatory molecules, and both JQ1 and GSK046 reduced the detection of most of these. Quantitative RT-PCR confirmed that both JQ1 and GSK046 reduced mRNA expression of a subset of these proinflammatory and additional profibrotic genes. While this supports that BET

proteins likely mediate proinflammatory/fibrotic gene expression, it remains unclear whether this reduction is a consequence of the diminished number of senescent cholangiocytes or directly related to BET protein function as a driver of proinflammatory/fibrotic gene expression in senescent cells. Importantly, the SASP has been implicated in paracrine induction of senescence, including in cholangiocytes,⁸ thus, further delineation of the role of BET proteins in proinflammatory/fibrotic gene expression may reveal how BD2 domain inhibition, while not promoting senescent cholangiocyte cell death, reduces cholangiocyte senescence *in vitro*.

The degree to which individual BET proteins differentially interact with regulatory complexes or play non-redundant roles in gene regulation has not been well characterized. We found that ETS1 formed an immunoprecipitable complex with both BRD2 and BRD4, yet the BRD2:ETS1 complex was more greatly increased in senescent cholangiocytes. Additionally, we demonstrated *in vivo*, with proximity ligation assays, that BRD2 interaction with ETS1 is increased in cholangiocytes of PSC patient tissue. Together, these data show that BRD2 and ETS1 interact and likely drive cholangiocyte senescence. Moreover, we found that RNAi depletion of BRD2 dramatically reduced expression of BCL-xL and p21. Hence, three pieces of data support a prominent role of BRD2 in mediating cholangiocyte senescence: i) cultured PSCDCs maintain the senescent phenotype with diminished BRD4 expression; ii) senescent cholangiocytes exhibit increased interaction between ETS1 and BRD2; and iii) depletion of BRD2 diminishes BCL-xL expression and suppresses cholangiocyte senescence. Thus, our data support that we've identified an essential molecular interaction between BRD2 and a senescence-associated transcription factor, ETS1, that promotes cholangiocyte senescence and may be exploited for therapeutic benefit in PSC.

We also demonstrated that BET protein inhibition in mouse models of cholestatic liver disease improved features of disease progression. These results support what has been found in other models of immune-mediated diseases¹³ and suggest a therapeutic role of BET protein inhibition in senescence-associated cholestatic liver diseases, including PSC. Our results also expose areas that require further exploration. Our cumulative data supports unique functions of the BD1 and BD2 domains; for example, only the dual BD1/BD2 inhibitor, JQ1, promoted senescent cholangiocyte cell death, yet both JQ1 and the selective BD2 inhibitor GSK046 reduced the abundance of senescent cholangiocytes *in vitro*. Importantly, it has been shown that selective inhibition of BD2 suppressed the induced expression of inflammatory genes and improved tolerability of BET inhibitors in animal models of inflammatory and autoimmune disease.¹³ These results suggest distinct, yet largely unexplored differences in BET protein bromodomains that may be exploited for therapeutic benefit. Our ongoing studies are focused on the non-redundant functions of BET proteins, with a focus on BRD2 and BRD4 in PSC pathogenesis and identifying unique functions of BET protein BD1 and BD2 domains.

In conclusion, we have defined that BET proteins are upregulated in senescent cholangiocytes and mediate this cellular fate *in vitro*. We provide further evidence that these proteins are upregulated in cholangiocytes in PSC patient tissue and provide evidence that inhibition of these proteins improves murine models of PSC. Our data also support a

major role of BRD2, and its interaction with ETS1, as essential transcriptional regulators *in vitro* and in murine models of biliary disease. These data support that targeted inhibition of BET proteins is an attractive novel therapy for PSC. Additionally, these results may be generalizable to other senescence-associated diseases, including atherosclerosis, osteoarthritis, non-alcoholic fatty liver disease, and idiopathic pulmonary fibrosis.

Supplementary Material

Refer to Web version on PubMed Central for supplementary material.

Acknowledgments

P30 DK084567 (NFL)

R01 DK057993 (NFL)

R01 DK0124182 (GJG)

PSC Partners Seeking a Cure (SPO)

Chris M. Carlos and Catharine Nicole Jockisch Carlos Endowment in PSC

Data statement:

Unique research resources generated by this project (including data, analytic methods, and study materials) will be available upon requests made to the corresponding author. Should any intellectual property arise which requires a patent, we will ensure that the technology (materials and data) remains widely available to the research community.

Abbreviations:

(BET)	Bromodomain and Extraterminal domain proteins
(BRD2)	Bromodomain containing 2
(BRD3)	Bromodomain containing 3
(BRD4)	Bromodomain containing 4
(FACS)	Fluorescence-activated cell sorting
(NHC)	Normal human cholangiocytes
(NHCsen)	NHC experimentally induced to senescence
(PSC)	Primary sclerosing cholangitis
(PSCDC)	PSC patient-derived cholangiocytes
(SA- β GAL)	Senescence-associated beta-galactosidase
(SASP)	Senescence-associated secretory phenotype

REFERENCES CITED

1. Karlsen TH, Folseraas T, Thorburn D, et al. Primary sclerosing cholangitis - a comprehensive review. *J Hepatol* 2017;67:1298–1323. [PubMed: 28802875]
2. Lazaridis KN, LaRusso NF. Primary Sclerosing Cholangitis. *N Engl J Med* 2016;375:2501–2502.
3. Bambha K, Kim WR, Talwalkar J, et al. Incidence, clinical spectrum, and outcomes of primary sclerosing cholangitis in a United States community. *Gastroenterology* 2003;125:1364–9. [PubMed: 14598252]
4. Alabraba E, Nightingale P, Gunson B, et al. A re-evaluation of the risk factors for the recurrence of primary sclerosing cholangitis in liver allografts. *Liver Transpl* 2009;15:330–40. [PubMed: 19243003]
5. Coppe JP, Desprez PY, Krtolica A, et al. The senescence-associated secretory phenotype: the dark side of tumor suppression. *Annu Rev Pathol* 2010;5:99–118. [PubMed: 20078217]
6. Hernandez-Segura A, Nehme J, Demaria M. Hallmarks of Cellular Senescence. *Trends Cell Biol* 2018;28:436–453. [PubMed: 29477613]
7. Tchkonja T, Zhu Y, van Deursen J, et al. Cellular senescence and the senescent secretory phenotype: therapeutic opportunities. *J Clin Invest* 2013;123:966–72. [PubMed: 23454759]
8. Tabibian JH, O'Hara SP, Splinter PL, et al. Cholangiocyte senescence by way of N-ras activation is a characteristic of primary sclerosing cholangitis. *Hepatology* 2014;59:2263–75. [PubMed: 24390753]
9. O'Hara SP, Splinter PL, Trussoni CE, et al. The transcription factor ETS1 promotes apoptosis resistance of senescent cholangiocytes by epigenetically up-regulating the apoptosis suppressor BCL2L1. *J Biol Chem* 2019;294:18698–18713. [PubMed: 31659122]
10. O'Hara SP, Splinter PL, Trussoni CE, et al. ETS Proto-oncogene 1 Transcriptionally Up-regulates the Cholangiocyte Senescence-associated Protein Cyclin-dependent Kinase Inhibitor 2A. *J Biol Chem* 2017;292:4833–4846. [PubMed: 28184004]
11. Hardy K, Mansfield L, Mackay A, et al. Transcriptional networks and cellular senescence in human mammary fibroblasts. *Mol Biol Cell* 2005;16:943–53. [PubMed: 15574883]
12. Sturmlechner I, Zhang C, Sine CC, et al. p21 produces a bioactive secretome that places stressed cells under immunosurveillance. *Science* 2021;374:eabb3420. [PubMed: 34709885]
13. Gilan O, Rioja I, Knezevic K, et al. Selective targeting of BD1 and BD2 of the BET proteins in cancer and immunoinflammation. *Science* 2020;368:387–394. [PubMed: 32193360]
14. Mohammad HP, Barbash O, Creasy CL. Targeting epigenetic modifications in cancer therapy: erasing the roadmap to cancer. *Nat Med* 2019;25:403–418. [PubMed: 30842676]
15. Wu SY, Chiang CM. The double bromodomain-containing chromatin adaptor Brd4 and transcriptional regulation. *J Biol Chem* 2007;282:13141–5. [PubMed: 17329240]
16. Zeng L, Zhou MM. Bromodomain: an acetyl-lysine binding domain. *FEBS Lett* 2002;513:124–8. [PubMed: 11911891]
17. Berthon C, Raffoux E, Thomas X, et al. Bromodomain inhibitor OTX015 in patients with acute leukaemia: a dose-escalation, phase 1 study. *Lancet Haematol* 2016;3:e186–95. [PubMed: 27063977]
18. Azad AI, Krishnan A, Troop L, et al. Targeted Apoptosis of Ductular Reactive Cells Reduces Hepatic Fibrosis in a Mouse Model of Cholestasis. *Hepatology* 2020;72:1013–1028. [PubMed: 32128842]
19. Filippakopoulos P, Qi J, Picaud S, et al. Selective inhibition of BET bromodomains. *Nature* 2010;468:1067–73. [PubMed: 20871596]
20. Gadd MS, Testa A, Lucas X, et al. Structural basis of PROTAC cooperative recognition for selective protein degradation. *Nat Chem Biol* 2017;13:514–521. [PubMed: 28288108]
21. Winter GE, Buckley DL, Paulk J, et al. DRUG DEVELOPMENT. Phthalimide conjugation as a strategy for in vivo target protein degradation. *Science* 2015;348:1376–81. [PubMed: 25999370]
22. Tabibian JH, Trussoni CE, O'Hara SP, et al. Characterization of cultured cholangiocytes isolated from livers of patients with primary sclerosing cholangitis. *Lab Invest* 2014;94:1126–33. [PubMed: 25046437]

23. Li Y, Xiang J, Zhang J, et al. Inhibition of Brd4 by JQ1 Promotes Functional Recovery From Spinal Cord Injury by Activating Autophagy. *Front Cell Neurosci* 2020;14:555591. [PubMed: 32982695]
24. Wang L, Wu X, Huang P, et al. JQ1, a small molecule inhibitor of BRD4, suppresses cell growth and invasion in oral squamous cell carcinoma. *Oncol Rep* 2016;36:1989–96. [PubMed: 27573714]
25. Wang L, Wu X, Wang R, et al. BRD4 inhibition suppresses cell growth, migration and invasion of salivary adenoid cystic carcinoma. *Biol Res* 2017;50:19. [PubMed: 28545522]
26. Lu Y, Ma W, Li Z, et al. The interplay between p16 serine phosphorylation and arginine methylation determines its function in modulating cellular apoptosis and senescence. *Sci Rep* 2017;7:41390. [PubMed: 28120917]
27. Faivre EJ, McDaniel KF, Albert DH, et al. Selective inhibition of the BD2 bromodomain of BET proteins in prostate cancer. *Nature* 2020;578:306–310. [PubMed: 31969702]
28. Cummin TEC, Cox KL, Murray TD, et al. BET inhibitors synergize with venetoclax to induce apoptosis in MYC-driven lymphomas with high BCL-2 expression. *Blood Adv* 2020;4:3316–3328. [PubMed: 32717030]
29. Hogg SJ, Newbold A, Vervoort SJ, et al. BET Inhibition Induces Apoptosis in Aggressive B-Cell Lymphoma via Epigenetic Regulation of BCL-2 Family Members. *Mol Cancer Ther* 2016;15:2030–41. [PubMed: 27406984]
30. Wyce A, Ganji G, Smitheman KN, et al. BET inhibition silences expression of MYCN and BCL2 and induces cytotoxicity in neuroblastoma tumor models. *PLoS One* 2013;8:e72967. [PubMed: 24009722]
31. Kirkland JL, Tchkonja T. Senolytic drugs: from discovery to translation. *J Intern Med* 2020;288:518–536. [PubMed: 32686219]
32. Wang E. Senescent human fibroblasts resist programmed cell death, and failure to suppress bcl2 is involved. *Cancer Res* 1995;55:2284–92. [PubMed: 7757977]
33. Moncsek A, Al-Suraih MS, Trussoni CE, et al. Targeting senescent cholangiocytes and activated fibroblasts with B-cell lymphoma-extra large inhibitors ameliorates fibrosis in multidrug resistance 2 gene knockout (*Mdr2*($-/-$)) mice. *Hepatology* 2018;67:247–259. [PubMed: 28802066]
34. Wakita M, Takahashi A, Sano O, et al. A BET family protein degrader provokes senolysis by targeting NHEJ and autophagy in senescent cells. *Nat Commun* 2020;11:1935. [PubMed: 32321921]
35. Tasdemir N, Banito A, Roe JS, et al. BRD4 Connects Enhancer Remodeling to Senescence Immune Surveillance. *Cancer Discov* 2016;6:612–29. [PubMed: 27099234]

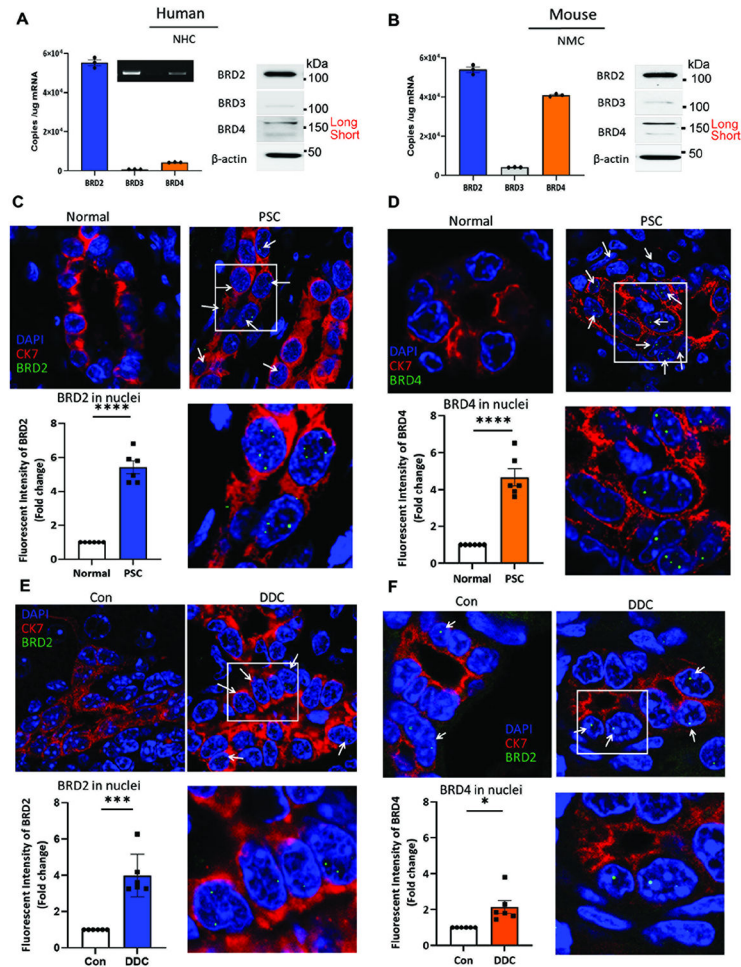


Figure 1. BET mRNA and proteins are expressed in human and mouse cholangiocytes. **A and B.** BET mRNA expression (copy number/microgram total mRNA) and protein expression (immunoblot) in normal human (A) and mouse (B) cholangiocytes. $n = 3$ independent experiments (images of blots are shown at similar membrane exposure times). **C-F.** Representative confocal images for DAPI (blue), CK19 (red), and BRD2 (C and E; green) or BRD4 (D and F; green) in cholangiocytes of normal and PSC human liver samples (C and D), and wild-type control (Con) and DDC-fed mouse livers (E and F). Arrows identify cells with positive nuclear expression of BET proteins (observed as puncta), outlined region is enlarged. Analysis of fluorescence intensity demonstrates increased BRD2 and BRD4 in PSC patient and DDC-fed mice cholangiocyte nuclei compared with respective non-disease controls. Fluorescence intensity was measured in six bile ducts from each condition and presented as mean fold-change \pm S.E.M.

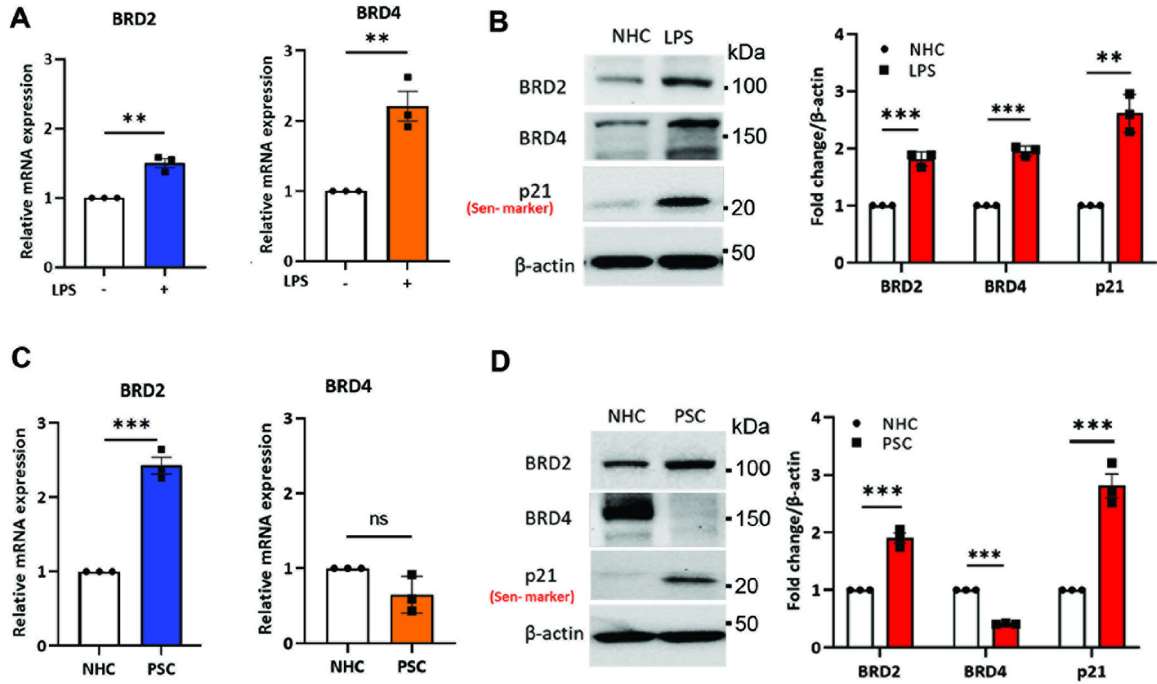


Figure 2. NHCs experimentally induced to senescence (NHCsen) and PSC patient-derived cholangiocytes (PSCDCs) exhibit increased BET expression.

A. mRNA expression was assessed by qPCR in NHC (no LPS) or NHCsen (LPS). NHCsen exhibited increased BRD2 (~1.5-fold) and BRD4 (~2.3-fold). **B.** Immunoblot analysis shows increased protein expression of BRD2 (~2-fold), BRD4 (~2-fold) and p21 (~2.5-fold) in NHCsen. $n = 3$ independent experiments. **C and D.** In PSCDCs (PSC), qPCR and immunoblots show increased expression of BRD2 mRNA (~2.5-fold) and protein (~2-fold); BRD4 mRNA expression was unchanged, while BRD4 protein was diminished compared to NHC. Immunoblots for p21 demonstrate increased senescence in PSCDCs ($n = 3$).

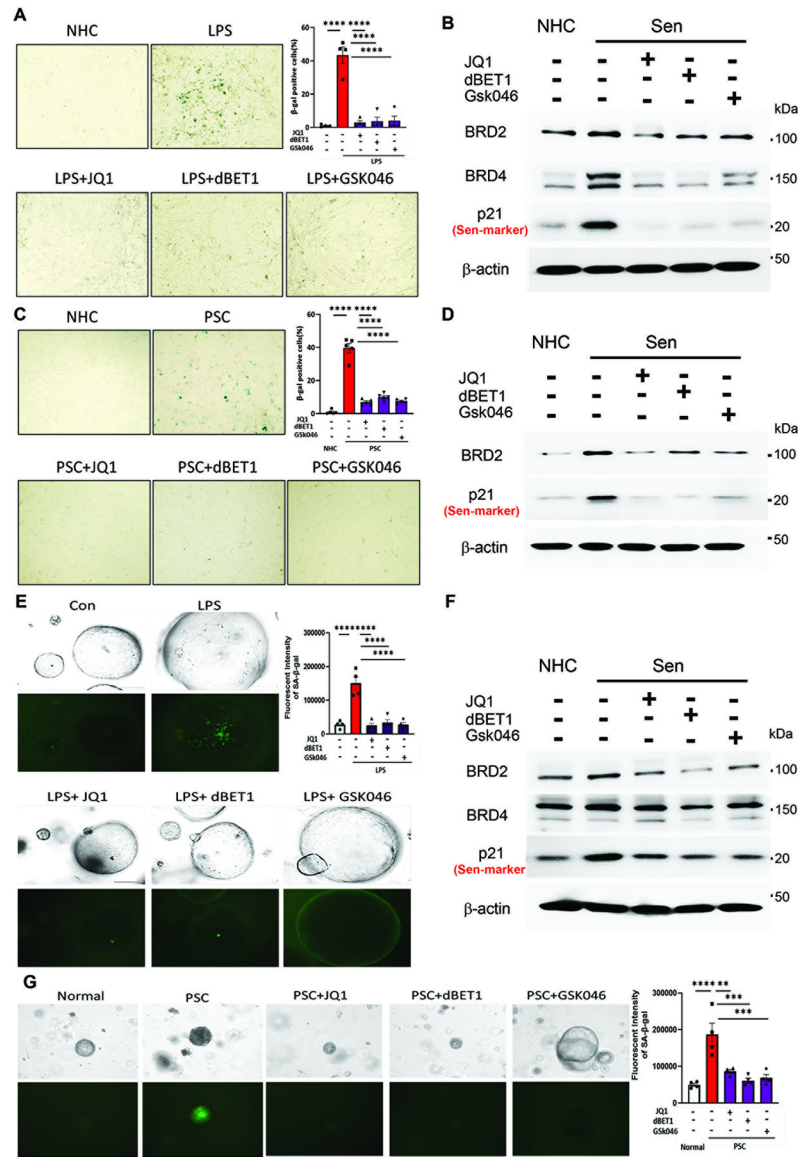


Figure 3. BET inhibitors decrease senescence in NHCsen and PSCDCs.

A-D. Control NHC (no LPS), NHCsen (LPS), and PSCDCs (PSC) were stained for SA- β -gal and immunoblots performed to assess senescence (p21) and BET protein expression. Approximately 40% of the NHCsen (**A**) and PSCDCs (**C**) exhibited SA- β -gal positivity. Following treatment with BET protein inhibitors (JQ1, dBET1, and GSK046), SA- β -gal positivity was observed in less than 10% of the cholangiocytes. $n = 5$ independent experiments. NHCsen exhibited increased BRD2, BRD4, and p21, while the BET protein inhibitors reduced their expression. (**B**). PSCDCs exhibited increased BRD2 and p21 compared to NHC control and the BET inhibitors reduced expression of both (**D**). Western blots shown are representative from 3 separate experiments. **E.** Non-cholestatic liver disease patient cholangiocytes were isolated from bile and grown as organoids, induced to senescence (LPS), and cultured in the presence/absence of BET inhibitors for 48 hours. Each BET inhibitor decreased SA- β -gal positivity as measured by fluorescent

intensity, $n = 3$ independent experiments. **F.** Immunoblots reveal that induced senescent cholangiocyte organoids exhibited increased BRD2, BRD4, and p21 protein expression compared to control cholangiocyte organoids. BET inhibitors reduced expression of each of these. **G.** Cholangiocytes isolated from PSC patient bile (PSC) were grown as organoids and exhibited increased SA- β -gal positivity compared to non-cholestatic liver disease patient cholangiocyte organoids (Normal); each BET inhibitor decreased PSC organoid SA- β -gal positivity, $n = 3$ independent experiments. Representative immunoblots from $n = 3$ independent experiments.

Author Manuscript

Author Manuscript

Author Manuscript

Author Manuscript

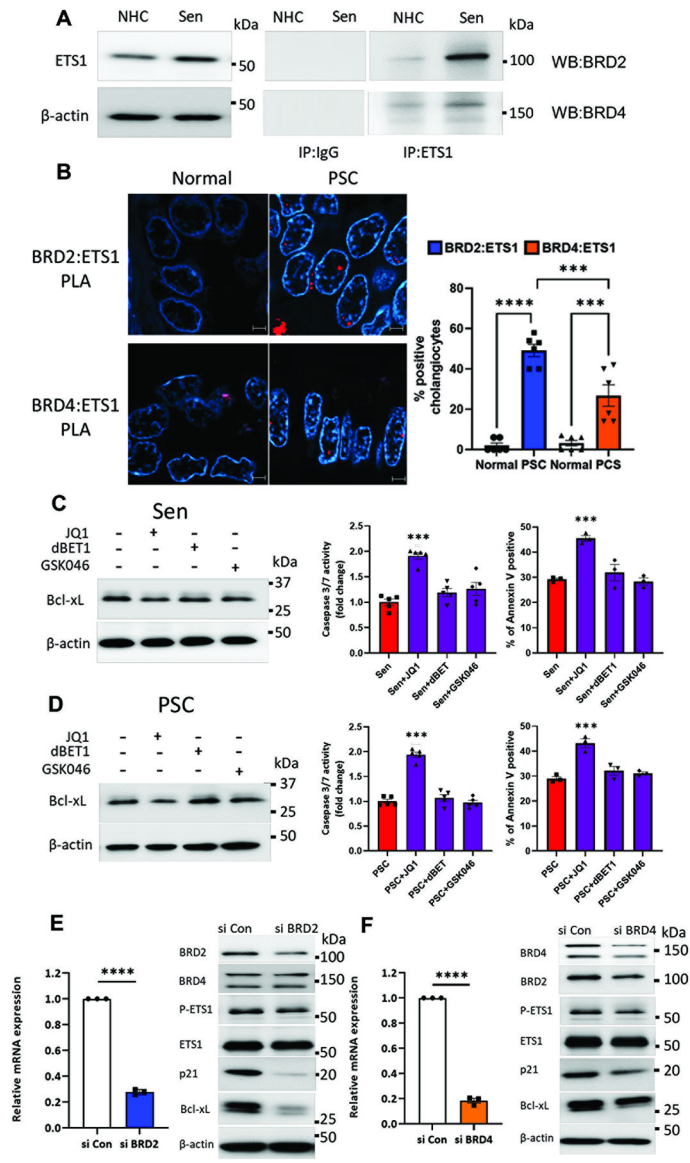


Figure 4. BET proteins interact with the transcription factor, ETS1, and the BET protein inhibitor, JQ1, promotes senescent cell apoptosis.

A. ETS1 forms an immunoprecipitable complex with the BET proteins, and this complex is increased (BRD2: ~20-fold and BRD4: ~2-fold) in NHCsen (Sen) compared to non-senescent cholangiocytes. **B.** Proximity ligation assays on PSC patient tissue demonstrated increased BRD2 and BRD4 interaction (red) with ETS1 in PSC cholangiocyte nuclei (blue). Quantitation reveals significantly increased BRD2:ETS1 versus BRD4:ETS1 interaction in PSC patient cholangiocytes. **C and D.** Both NHCsen (Sen, **C**) and PSCDCs (PSC, **D**) were cultured in the presence or absence of BET inhibitors. Immunoblot analysis shows that BCL-xL is expressed in both NHCsen and PSCDCs; expression of BCL-xL is diminished in the presence of JQ1 in both NHCsen (35%) and PSCDCs (40%). Western blots shown are representative from 3 separate experiments. Apoptosis, measured by caspase-3/7 assay and Annexin V positivity, is increased in JQ1 treated NHCsen (**C**) and PSCDCs (**D**) (~2-fold). $n = 3$ for immunoblot and $n = 5$ caspase-3/7 and Annexin V assays. **E and F.** FACS sorted

NHCsen were transfected with either control (siCon), BRD2 (siBRD2), or BRD4 (siBRD4) siRNAs. Knockdown of BRD2 or BRD4 was confirmed by qPCR and immunoblot. Additional immunoblots show that both BRD2 and BRD4 suppression diminishes phospho-ETS1 expression. RNAi suppression of BRD2 suppressed both BCL-xL and p21 expression, while RNAi-mediated suppression of BRD4 only slightly diminished BCL-xL and p21 expression, β -actin used as a loading control. $n = 3$ independent experiments.

Author Manuscript

Author Manuscript

Author Manuscript

Author Manuscript

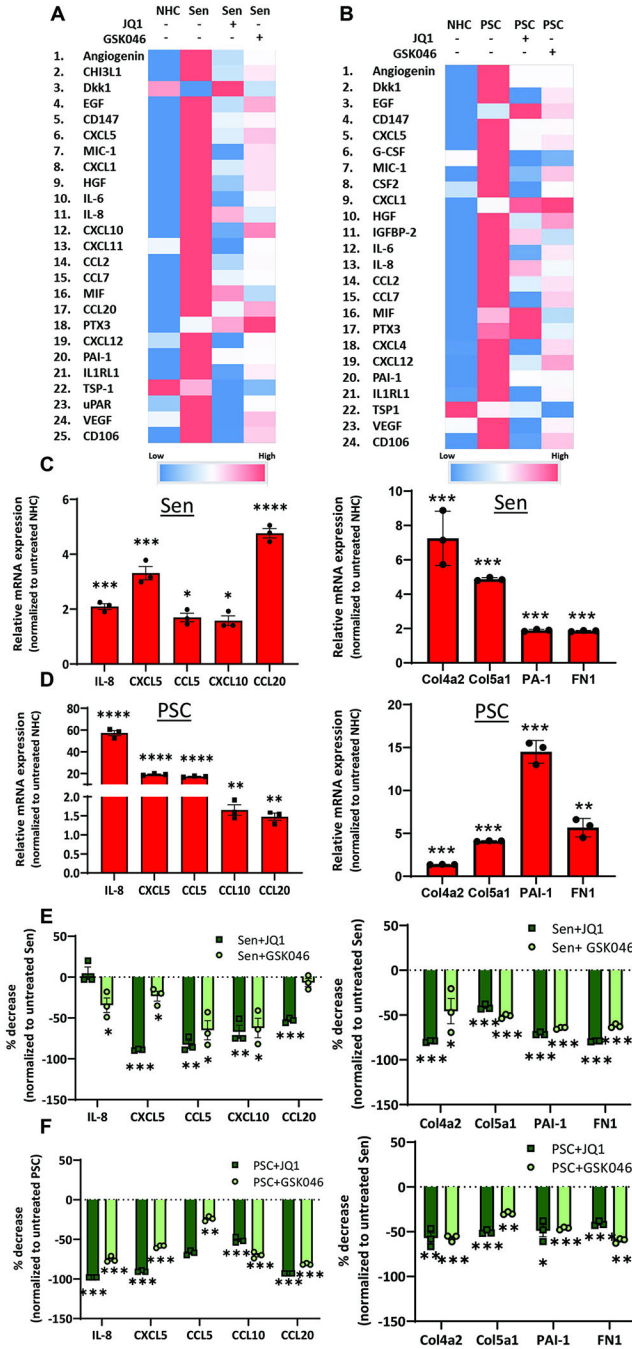


Figure 5. BET inhibitors suppress the senescent cell bioactive secretome and expression of proinflammatory/fibrogenic genes.

A. Multiplex antibody array detected cytokines and chemokines in conditioned media from NHC, NHCsen (Sen), or NHCsen treated with JQ1 or GSK046. The heat map represents quantification of each analyte on an arbitrary scale from low to high pixel intensity. NHCsen showed increased secretion of 22 of the 105 proinflammatory/fibrogenic analytes compared to NHC; treatment with the BET inhibitors reduced the majority (>90%) of these analytes. **B.** PSCDCs exhibited increased secretion of 21 of the 105 analytes compared to NHC, ~80% of which overlapped with the NHCsen secretome profile; the majority (>90%) were

reduced by BET inhibitors. **C.** Proinflammatory and fibrogenic mRNA expression assessed by qPCR in NHCsen (Sen) showed increased proinflammatory (IL-8, CXCL5, CXCL10 and CCL20) gene expression (~2–4.5-fold) and increased profibrogenic (COL4A2, COL5A1, PAI-1 and FN1) gene expression (~2–7-fold) compared to NHC control. **D.** PSCDCs (PSC) exhibited increased mRNA expression of the chemokines (~1.5- 60-fold) and profibrogenic genes (~2-15-fold) compared to NHC control. n= 3 independent experiments. **E.** In NHCsen, JQ1 reduced the expression of 4/5 chemokines (50-90%); GSK046 reduced the expression of 4/5 chemokines (25-60%). Both JQ1 and GSK046 reduced the expression of the profibrogenic genes (~50-90%). **F.** In PSCDCs, JQ1 and GSK046 reduced the expression of proinflammatory (~25-90%) and fibrogenic genes (~40-90%) compared to NHC control.

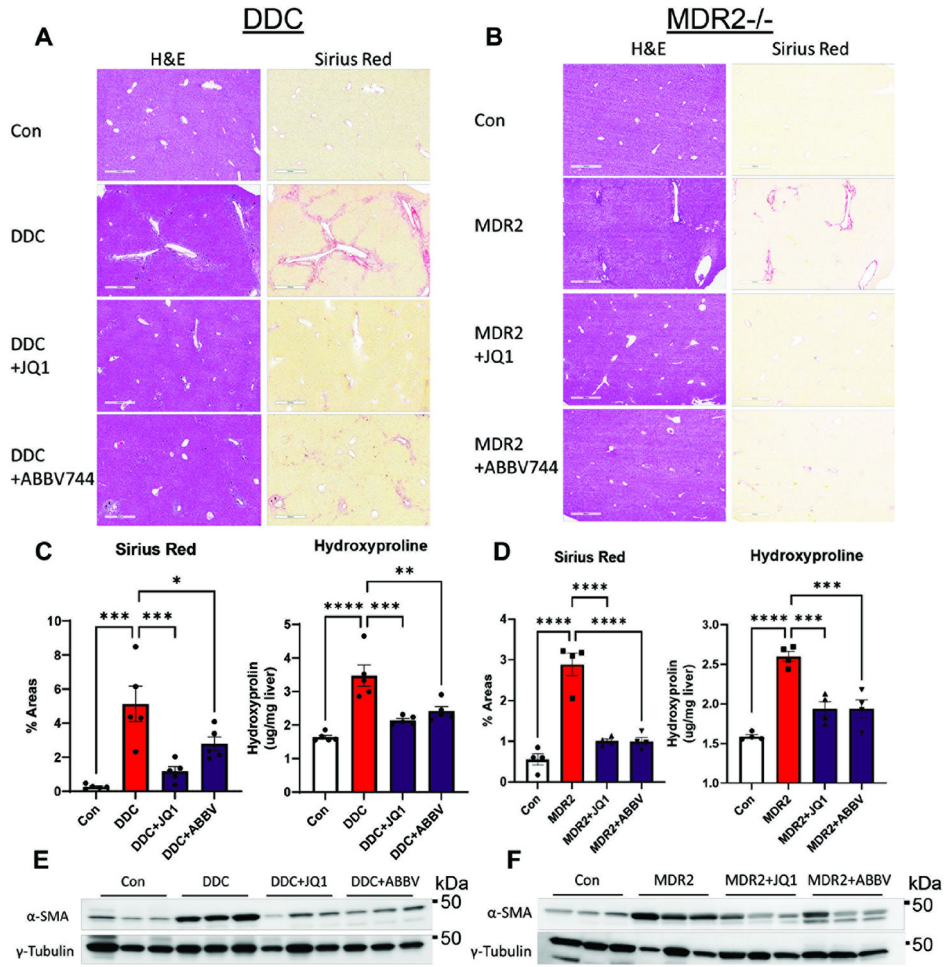


Figure 6. BET inhibitors diminish fibrosis in the DDC-fed and *Mdr2*^{-/-} mouse models of sclerosing cholangitis.

A. Representative images of H&E-stained liver sections (magnification: 40×) showing parenchyma and portal tracts of wild-type control (Con), DDC-fed, and DDC-fed BET inhibitor treated mice (left panels) and Picrosirius-red-stained liver sections (magnification: 40×) showing deposition of collagen (right panels). Quantitation of Picrosirius (**C**) reveals a significant reduction in fibrosis in BET inhibitor-treated mice. Data is presented as the percentage of Picrosirius positive/ total liver area. **B.** Representative H&E images of wild-type control (Con), *Mdr2*^{-/-}, and *Mdr2*^{-/-} BET inhibitor treated mice (left panels) and Picrosirius-red-stained liver sections (magnification: 40×, right panels). Picrosirius-red quantitation (**D**) reveals significant reduction in fibrosis in BET inhibitor-treated *Mdr2*^{-/-} mice. Hydroxyproline assay confirmed decreased collagen content following BET inhibitor treatment in the DDC-fed (**C**) and *Mdr2*^{-/-} mice (**D**). Bars represent mean ± SEM; n = 5 mice/ group for DDC experiments and n=4 mice for *Mdr2*^{-/-} experiments. **E and F.** Immunoblotting of α-SMA from total liver lysates showed reduced expression of this myofibroblast marker following BET inhibitor treatment in both DDC-fed (**E**) and *Mdr2*^{-/-} mice (**F**).

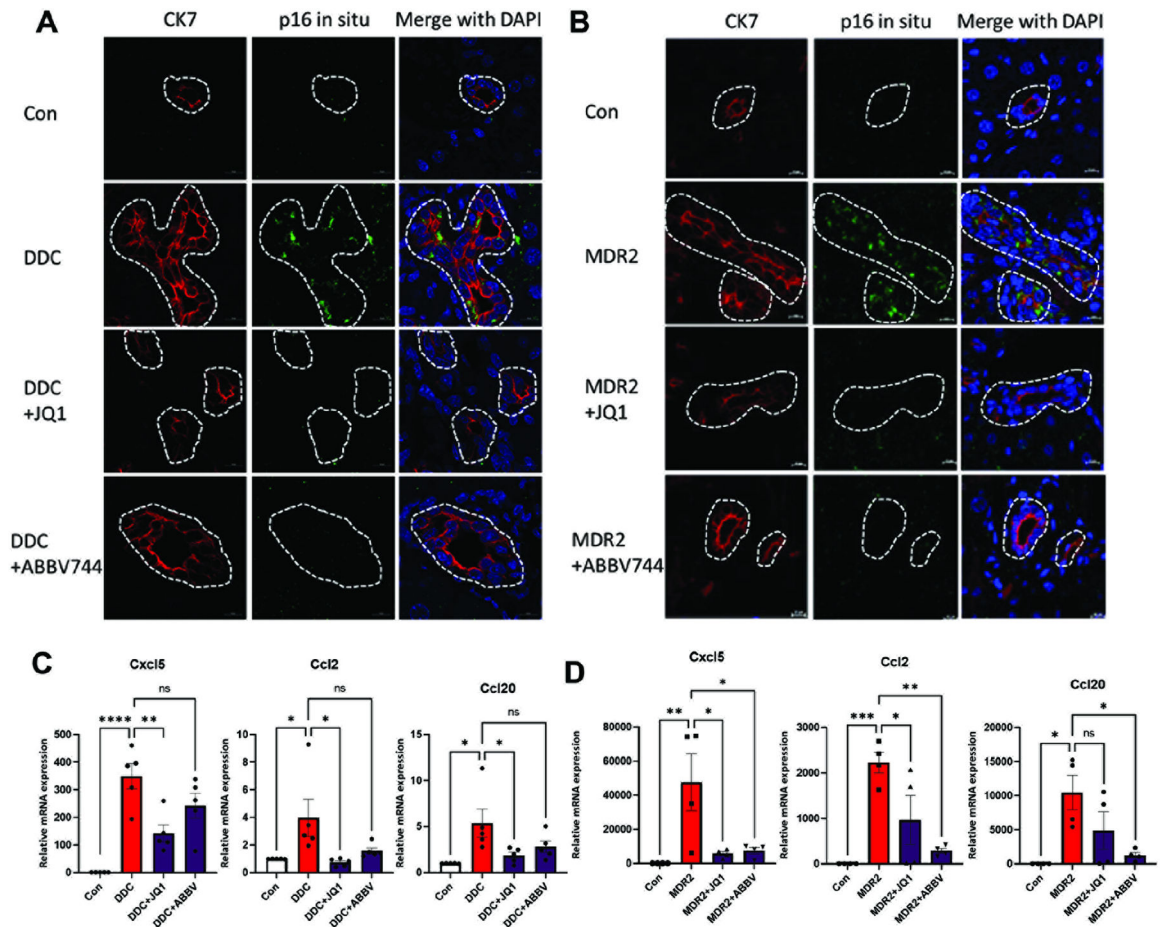


Figure 7. BET inhibitors diminish cholangiocyte senescence and proinflammatory gene expression in DDC-fed and *Mdr2*^{-/-} mouse models of sclerosing cholangitis.

A. Representative confocal images for CK7 (red), p16-in situ hybridization (green), DAPI (blue) in cholangiocytes of control, DDC-fed, and DDC-fed mice treated with BET inhibitors. DDC-fed mice exhibit increased p16 expression compared to control mice, which is reduced with BET inhibitor treatment. **B.** Representative confocal images for CK7 (red), p16-in situ hybridization (green), DAPI (blue) in cholangiocytes of control wild-type, *Mdr2*^{-/-}, and *Mdr2*^{-/-} mice treated with BET inhibitors. *Mdr2*^{-/-} mice exhibit increased p16 expression, which is reduced in BET inhibitor treated mice. **C.** RT-PCR, using whole liver lysate, demonstrated that DDC-fed mice exhibit increased proinflammatory gene expression of the SASP markers (CXCL5, CCL20 and CCL2), which is reduced by JQ1. DDC-fed ABBV744 treated mice exhibit a trend towards reduction of these inflammatory markers. **D.** RT-PCR using whole liver lysates, demonstrated that *Mdr2*^{-/-} mice exhibit increased proinflammatory gene expression; both JQ1 and ABBV744 reduced expression of these inflammatory genes. Bars represent mean \pm SEM; n = 5 mice/ group for DDC experiments and n=4 mice for *Mdr2*^{-/-} experiments.